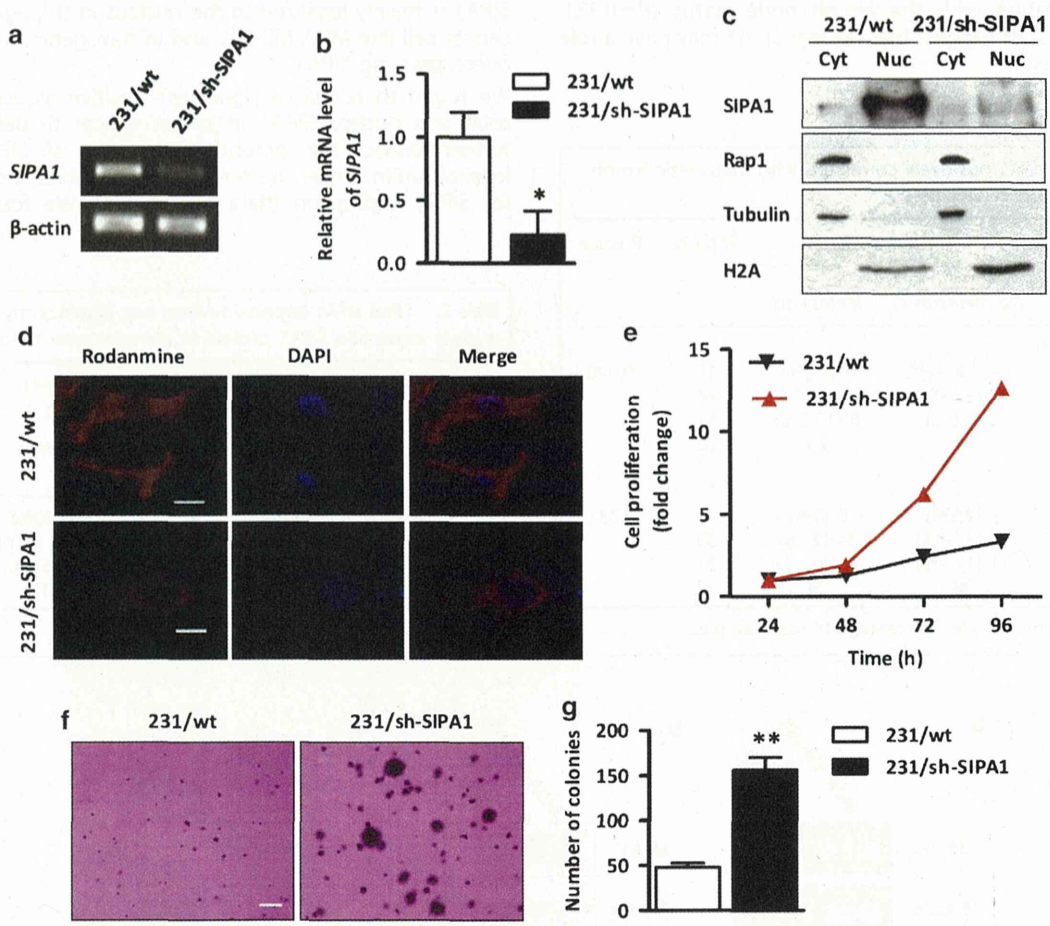


**Figure 3.** Knockdown of SIPA1 in MDA-MB-231 alters cell morphology and proliferation. (**a**, **b**) The mRNA levels of SIPA1 in 231/wt and 231/sh-SIPA1 cells were determined by RT–PCR and real-time PCR using 1 μg mRNA extracted from cells. (**c**) 231/wt and 231/sh-SIPA1 cells were cultured for 48 h followed by fractionation and immunoblotting with anti-SIPA1 and anti-Rap1antibodies. α-Tubulin and H2A were used as loading and fractionation controls. (**d**) Cells were seeded on the cover slips and stained with an anti-F-actin antibody and DAPI. Fluorescent images were taken with a confocal microscope. Scale bar, 10 μm for 231/wt and 5 μm for sh-SIPA1. (**e**) Cells were grown in 24-well plates, and absorbance values were measured at the indicated time points. (**f**) 231/wt and 231/sh-SIPA1 cells were cultured in the soft-agar plates. After 18 days, the colonies were stained with crystal violet and photographed. Scale bar, 100 μm. The numbers of colonies in each plate from the triplicates were counted and statistically analyzed (**g**).

exhibited high mRNA and protein expression in the highly invasive and metastatic human breast cancer cell MDA-MB-231 but low expression in the MCF7 cell line (Figures 2a and b). Consistent with our observation in tissue, we found that SIPA1 mainly localized in MDA-MB-231 to the cell nucleus (Figures 2c and d). To study the presence of SIPA1 in the nuclear fraction as a physiological phenomenon, we used stimuli such as FBS, fibronectin and Matrigel. This revealed that SIPA1 was mainly localized in the cytoplasm in the absence of an external stimulus and was present in the nucleus upon treatment with FBS or fibronectin (Figure 2e). To further confirm the nuclear localization of SIPA1 in breast cancer cells, we introduced the *SIPA1* gene into MCF7 cells, which has low endogenous levels of expression of SIPA1, to overexpress its protein (Figure 2f) and found that increased SIPA1 expression mostly occurred in the nucleus (Figure 2g).

### Knockdown of SIPA1 in MDA-MB-231 alters cell morphology and proliferation

To explore SIPA1's roles during breast cancer progress, endogenous *SIPA1* gene expression was stably silenced by a retrovirus-mediated shRNA approach in the MDA-MB-231 cell line. RT–PCR, real-time PCR and immunoblotting on fractionated samples were performed to confirm the decreased expression of SIPA1 in the MDA-MB-231 cell line (231/sh-SIPA1). SIPA1 mRNA level decreased by 70% compared with wild-type cells (231/wt) (Figures 3a and b), primarily because of a decrease in nuclear SIPA1 protein levels (Figure 3c). In addition, we found that Rap1 was mainly localized in cytoplasm regardless of SIPA1 level in 231 cells, implying that SIPA1 knockdown would likely only have a limited effect on Rap1 function in the cytoplasm. While culturing the cells, we noticed that SIPA1-suppressed cells rounded and lost the typical epithelioid morphology of MDA-MB-231 cells. Immunofluorescent staining with an anti-F-actin antibody followed by confocal imaging revealed a decreased formation of lamellipodia or invadopodia (Figure 3d). Next, we compared the proliferation ability of the two cells and found that knockdown of SIPA1 expression increased MDA-MB-231 cell proliferation *in vitro*, as well as anchorage-independent growth (Figures 3e and f). These results suggested an enhanced tumor-initiating capability in 231 cells upon SIPA1 knockdown.

### SIPA1 drives the adhesion, migration and invasion of MDA-MB-231 cells

As SIPA1 has been reported to be involved in regulating cancer cell adhesion,[16,21,22] we compared the adhesion ability of 231/wt and 231/sh-SIPA1 cells to both ECM and endothelial cells. This showed that suppression of SIPA1 decreased the ability of cells to adhere to ECM in Matrigel-treated plates (Figure 4a). Consistent

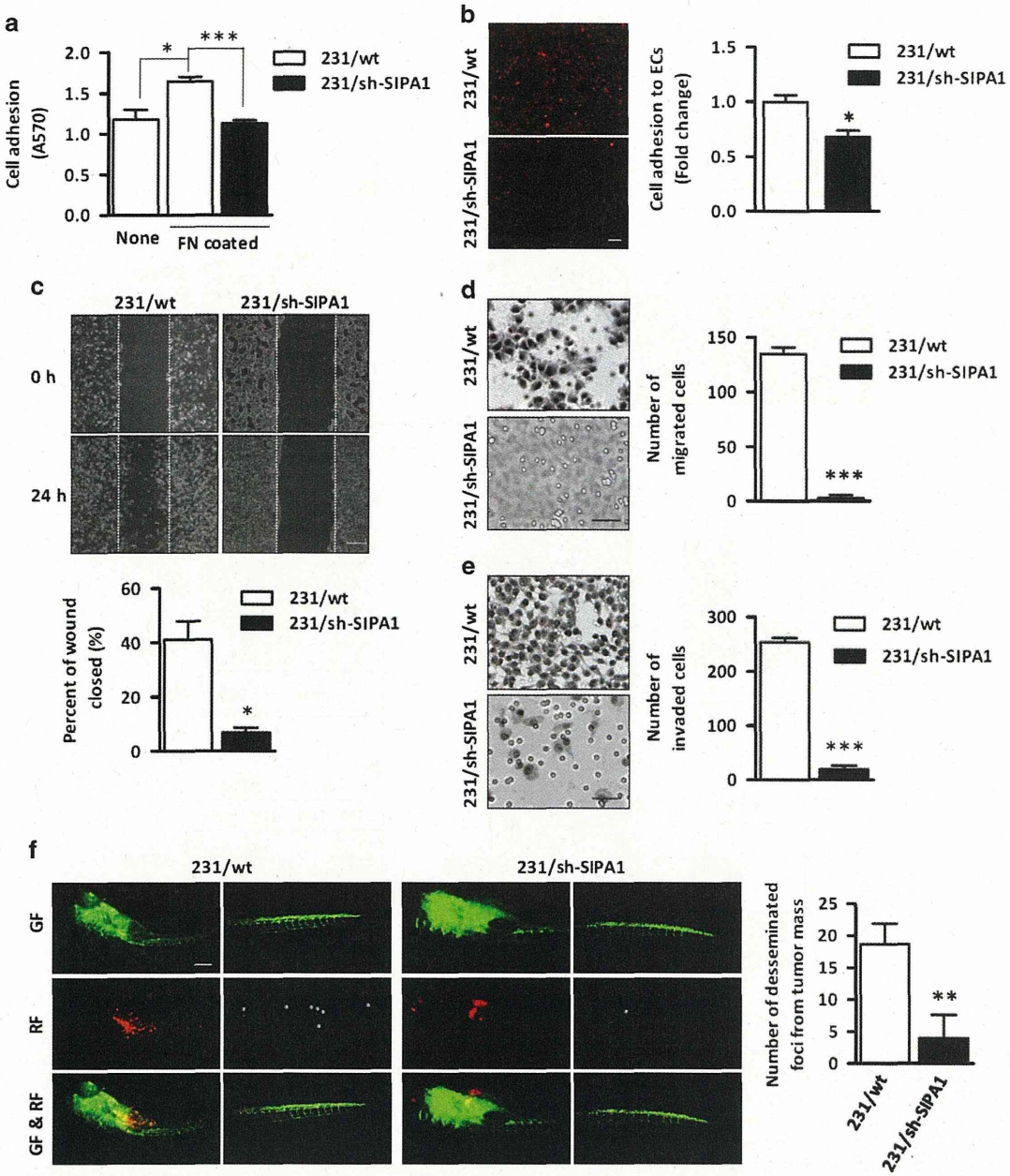


**Figure 4.** SIPA1 drives the adhesion, migration and invasion of MDA-MB-231 cells. (**a**) A total of $1 \times 10^5$ of 231/wt and 231/sh-SIPA1 cells suspended in serum-free media were plated onto culture wells with the indicated treatment for 30 min, and adherent cells were quantified at A570 after staining with crystal violet. (**b**) HUVECs were seeded into six-well plate 48 h before adding Dil-labeled 231/wt and 231/sh-SIPA1 cells. After co-incubating at 37 °C for 30 min, adherent cells were visualized by fluorescence imaging (left). Fluorescence intensities of the images were measured by Image J software and normalized to cell morphology, respectively. The mean ± s.d. are shown (right). Scale bar, 200 μm. (**c**) Cells were cultured in a six-well plate until reaching greater than 90% confluence. A scratch was made with a pipet in each well, and cells were photographed after 24 h (left). Quantification of the scratch image was performed by calculating the percent of the area covered with migrated cells (right). Scale bar, 200 μm. (**d**) Transwell migration assay. A total of $1 \times 10^5$ of cells were seeded into each chamber and incubated at 37 °C for 24 h. Representative photos are shown (left). Data presented are the mean of triplicate replications, and s.d. is indicated by error bars (right). Scale bar, 100 μm. (**e**) Transwell invasion assay. The inserts in the chamber were coated with Matrigel for 1 h before seeding cells. After incubation for 6 h, transmigrated cells were stained and representative photos are shown (left). Shown are the averages and s.d. (right). Scale bar, 100 μm. (**f**) Dil-labeled 231/wt and 231/sh-SIPA1 cells were injected into the perivitelline space of 48-hour post-fertilization embryos and tumor cell invasion, dissemination and metastasis were detected using fluorescent microscopy at day 6 postinjection. White asterisks indicate disseminated tumor foci. GF, green fluorescence; RF, red fluorescence. Quantification of numbers of disseminated tumor foci ($n = 3$ per group). Scale bar, 200 μm.

with this, the number of Dil-labeled 231/sh-SIPA1 cells that adhered to HUVECs seeded on a 24-well plate was significantly lower than the number of 231/wt cells that adhered in a control experiment (Figure 4b). On the basis of the observation that nuclear-positive SIPA1 correlated with metastatic lymph node status in breast cancer patients, SIPA1's effects on cell invasion and migration were further assayed. Using a standard scratch assay, 231/wt cells were seen to migrate into a wounded region after culturing 24 h; however, few 231/sh-SIPA1 cells in the scratched region were observed (Figure 4c), suggesting that

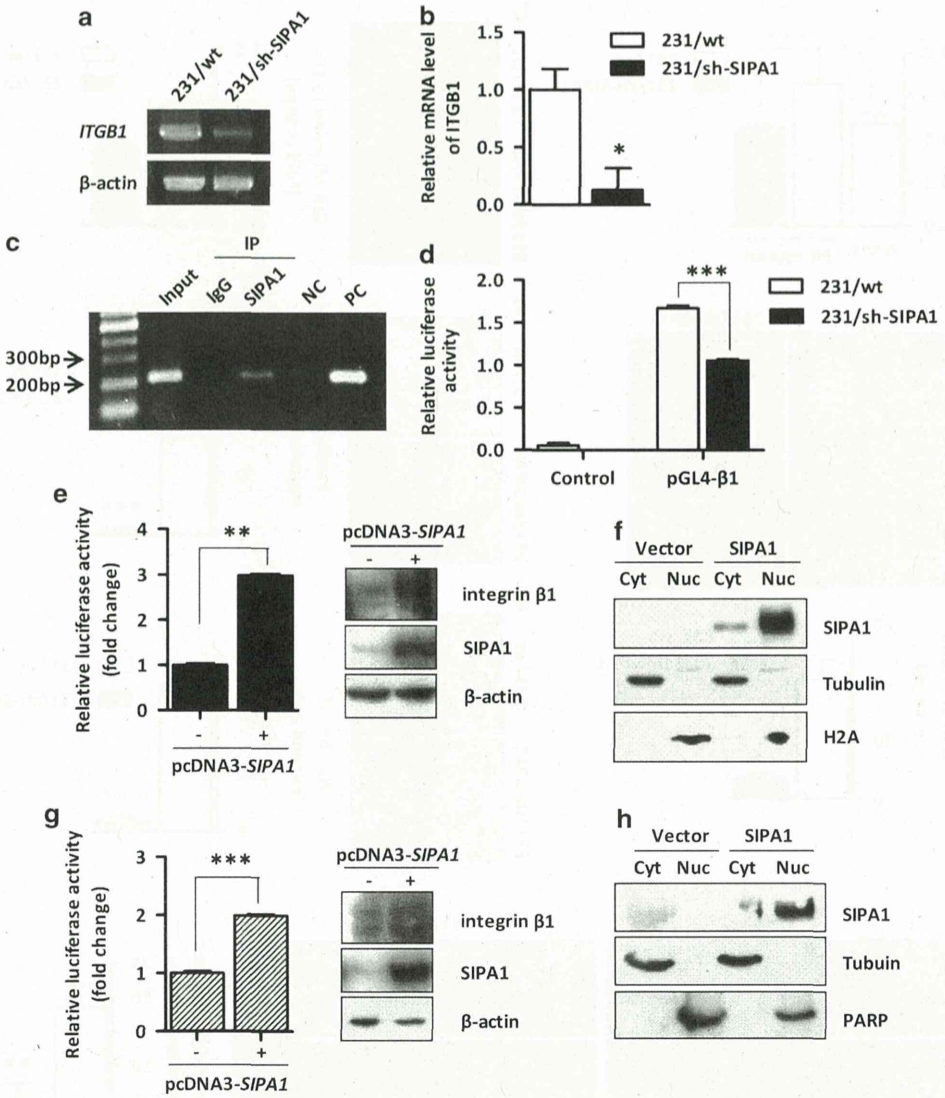


**Figure 5.** Nuclear SIPA1 interacts with and activates the integrin β1 promoter. The mRNA level of ITGB1 in 231/wt and 231/sh-SIPA1 cells was measured using RT–PCR (**a**) and real-time PCR (**b**). (**c**) SIPA1 binding to the promoter of β1 integrin gene was assayed by ChIP. Crosslinked nuclear extracts of MDA-MB-231 cells were immunoprecipitated by either an anti-SIPA1 antibody or a normal mouse IgG. Genomic DNA of MDA-MB-231 cells and water were used as positive (PC) and negative controls (NC) in the PCR. (**d**) Transcription activity of *ITGB1* promoter. 231/wt and 231/sh-SIPA1 cells were transfected with pGL-4-β1 or vector only (control). A Renilla plasmid was cotransfected as well. Forty-eight hours later, cells were lysed and relative luminescence was analyzed. (**e**) 231/sh-SIPA1 cells transfected with *SIPA1* gene were used for a luciferase reporter assay (left). Gene expression was confirmed by immunobloting with indicated antibodies (right). (**f**) 231/sh-SIPA1 cells transfected with *SIPA1* gene were subjected to cell fraction analysis. (**g**) HEK293 cells transfected with *SIPA1* gene were tested with a luciferase reporter assay (left). Gene expression was confirmed by immunobloting with indicated antibodies (right). (**h**) HEK293 cells transfected with *SIPA1* gene were subjected to cell fraction analysis.

knocking down SIPA1 expression suppressed MDA-MB-231 cells' migration. A transwell experiment was conducted to confirm that 231/sh-SIPA1 cells migrated less than wild-type cells on either uncoated or Matrigel-coated plates (Figures 4d and e). In addition, we employed a zebrafish xenotransplantation model to test the *in vivo* effect of the SIPA1 knockdown on cell migration.[23] DiI-labeled cells were injected into the perivitelline space of postfertilized 48-hour embryos and then scored for the dissemination of tumor cells after 6 days of incubation. The 231/sh-SIPA1 cells were primarily observed in the location of the yolk, while 231/wt cells were widely dispersed at the tail region (Figure 4f), indicating that SIPA1 knockdown reduced cell invasion and migration in zebrafish. Taken together, these data suggest that SIPA1 expression levels affect the invasive behavior of human tumor cells *in vitro* and *in vivo*.

### Nuclear SIPA1 interacts with and activates the integrin β1 promoter

Previous studies have shown that cell surface molecules such as CD44, CDHs, integrins and uPAR have important roles in cell adhesion, migration and invasion.[24–26] We investigated SIPA1-mediated transcriptional control of ITGB1, an integrin known to have important roles in cell adhesion and invasion. We found ITGB1 was significantly downregulated at the mRNA level in 231/sh-SIPA1 cells compared with the control 231/wt cells (Figures 5a and b and Supplementary Figure 1). We hypothesized that SIPA1 protein directly associates with the *ITGB1* gene and affects its transcription. A chromatin immunoprecipitation experiment was designed to examine the interaction of SIPA1 and the *ITGB1* promoter region. This promoter region was specifically amplified from MDA-MB-231 genomic DNA after immunopecipitated with

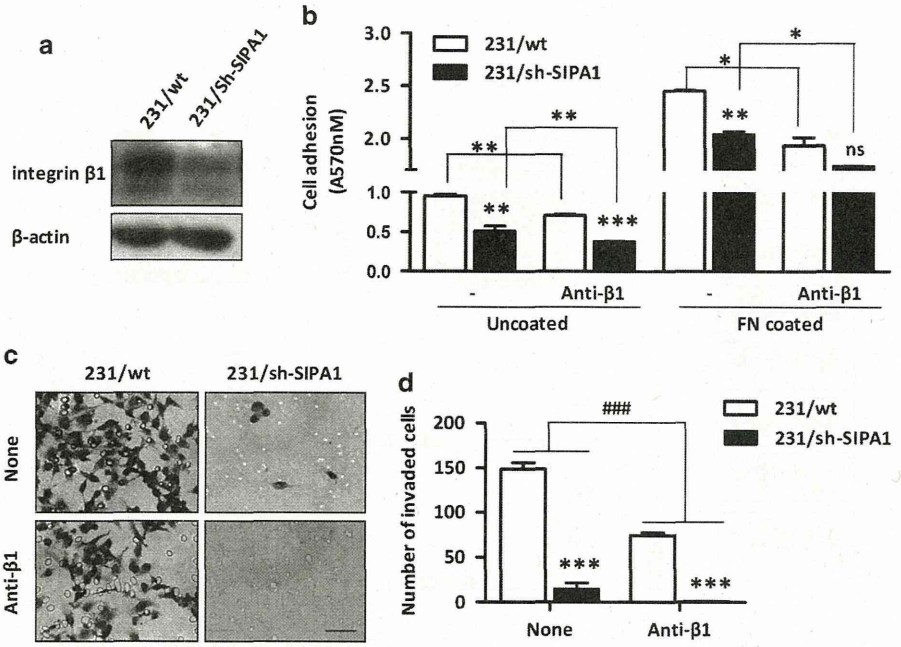


**Figure 6.** SIPA1 regulates breast cancer cell adhesion and invasion via integrin β1. (**a**) Whole-cell lysates of both cells were assayed by immunobloting to assess the protein level of integrin β1. (**b**) 231/wt and 231/sh-SIPA1 cells were pre-treated with either a 5 μg/ml antibody against integrin β1 for 2 h or IgG control, then equal amount of cells were seeded onto FN-coated or uncoated plates for a cell adhesion assay. (**c**) After treatment with an anti-β1 antibody, cells were seeded in FN-coated Transwell inserts followed by incubation at 37 °C for 6 h, transmigrated cells were stained and photographed. Scale bar, 100 μm. Shown are the averages and s.d. (**d**). $^{###}P < 0.001$, two-way analysis of variance analysis.

an anti-SIPA1 antibody (Figure 5c). In addition, a luciferase reporter gene assay was used to assess the impact of SIPA1 protein on *ITGB1* promoter transcriptional activity. We found that when *ITGB1* promoter sequence was cloned into a luciferase expression vector, luciferase activity was reduced in the 231/sh-SIPA1 cells (Figure 5d). Furthermore, overexpression of SIPA1 protein via transfection of the *Sipa1* gene (pcDNA3-*SIPA1*) into 231/sh-SIPA1 cells or HEK293 (confirmed by western blot for each line) cells increased *ITGB1* promoter transcriptional activity by two- to threefolds (Figures 5e and g). Consistently, the overexpressed SIPA1 in 231/sh-SIPA1 and HEK293 cells was mainly localized in their respective cell nuclei (Figures 5f and h). These results suggest that nuclear SIPA1 may bind to the *ITGB1* promoter and increase its transcription activity.

### SIPA1 regulates breast cancer cell adhesion and invasion via integrin β1

We saw that both 115 kDa and 130 kDa integrin β1 were markedly decreased at the protein level in 231/sh-SIPA1 cells compared with 231/wt control cells (Figure 6a). As integrin β1 is one of the major receptors of the ECM glycoprotein fibronectin,[27,28] we performed cell adhesion assays on fibronectin-treated surfaces. The results showed that on fibronectin-coated plates 231/wt control cells exhibited increased adhesion, and 231/sh-SIPA1 cells had decreased adhesion compared with wild-type cells. When the cells were treated with an anti-integrin β1 antibody, 231/sh-SIPA1 cells exhibited no significant decrease in adhesion ability towards fibronectin compared with that of wild-type cells (Figure 6b). A transwell assay using fibronectin as a coating reagent showed that an anti-integrin β1 antibody pre-treatment inhibited both 231/wt control and 231/sh-SIPA1 cell invasion (Figures 6c and d). However, the number of wild-type cells able to invade was higher than that of 231/sh-SIPA1 cells, even when the wild-type cells were incubated with an anti-integrin β1 antibody, implying that SIPA1 knockdown could affect integrin β1-related cell adhesion and invasion.

### SIPA1-knocked down MDA-MB-231 has impaired integrin-mediated FAK/Akt-MMP9 signaling pathway

On the bais of analysis of integrin-mediated cell adhesion and invasion, FAK is known to be phosphorylated by integrin-fibronectin ligation, a process that initiates a cascade of downstream signals leading to multiple adhesion and cytoskeletal changes.[29,30] Given our observations that 231/sh-SIPA1 cells exhibit poor attachment even on fibronectin-coated plates, and that integrin β1 expression is markedly decreased in this knockdown, we compared the phosphorylation of FAK, Akt and MMPs in 231/sh-SIPA1 cells to that in 231/wt cells by western blotting. Consistent with a role in the regulation of attachment, the SIPA1 knockdown cells exhibited decreased FAK and AKT phosphorylation with there was no obvious change of Src and ERK phosphorylation (Figure 7a). Previous studies have already shown that integrin β1 promotes cell invasion through upregulation of MMP9 as well as MMP2, collagenases that degrade ECM components in the tumor microenvironment.[31–33] We found that when SIPA1 is knocked down, mRNA levels of MMP9, but not MMP2, markedly decreased (assayed by either RT–PCR or real-time PCR) compared with 231/wt control cells (Figures 7b and c). The secreted MMP9 concentration in the culture medium of the 231/sh-SIPA1 cells, as measured by an ELISA assay, was much lower than in that of 231/wt control cells (Figure 7d), and a zymography assay showed that the proteolysis activity of MMP9 in the culture medium exhibited weaker enzymatic activity than control cells, while MMP2 showed no difference in enzyme activities in either line (Figure 7e). To discern whether MMP9 activity may have a role in this cell line in the observed decrease in cell invasion in the presence of decreased SIPA1 levels, an MMP9 inhibitor was assayed at increasing concentrations. An inhibitive effect on 231 cell invasion was found when 20 μM MMP9 inhibitor was present in the medium (Figure 7f). Also consistent with their being functional interplay between SIPA1 and MMP9 expression, we found that expression of both SIPA1 and MMP9 at the mRNA level was high in tumor and low in adjacent region of the assayed

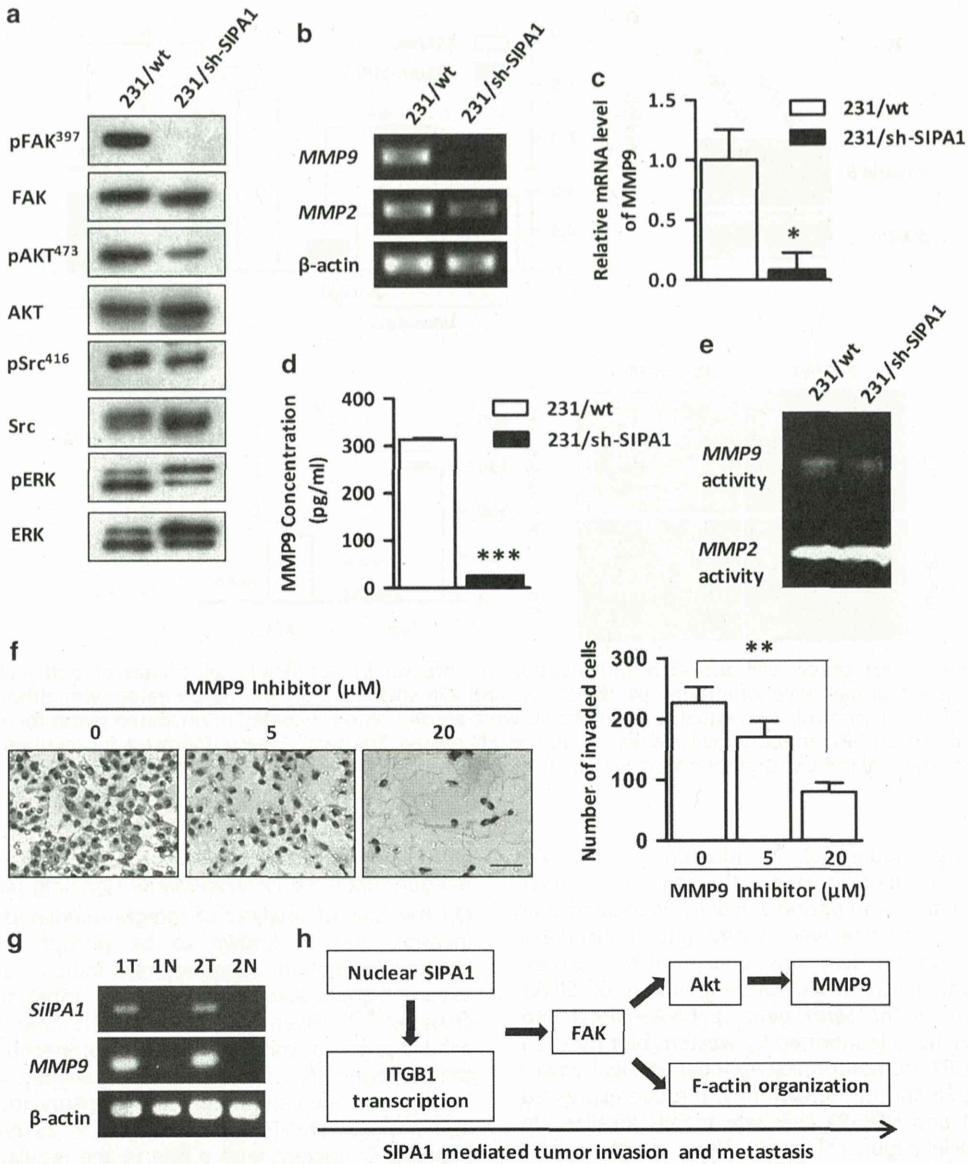


**Figure 7.** SIPA1-knocked down MDA-MB-231 has impaired integrin-mediated FAK/Akt-MMP9 signaling pathway. (**a**) Signaling molecules influenced by SIPA1 knockdown in MDA-MB-231 cells were assessed by western blot. After culturing for 48 h, mRNA levels of MMP9 in 231/wt and 231/sh-SIPA1 cells were assayed by RT–PCR (**b**) and real-time PCR (**c**). (**d**) Conditioned media of both cells was collected and subjected to an MMP9 Elisa analysis. The concentration of MMP9 was calculated accordingly based on a standard curve. (**e**) Enzyme activity of secreted MMP9 in conditioned media was analyzed by using zymography assay. (**f**) Cells were treated with an MMP9 inhibitor (MMP9 I) with the indicated concentration for 2 h followed by a transwell invasion assay. Representative photos are shown. Scale bar, 100 μm. Shown are the averages and s.d. (right). (**g**) RT–PCR analysis of freshly resected tissue samples. Representative results for the tumor (T) and corresponding normal (N) tissue are shown. (**h**) Proposed model of how SIPA1 regulates breast cancer cell adhesion, invasion and metastasis.

surgical specimens (Figure 7g). A model of how nuclear SIPA1 may act to promote breast cancer cell adhesion, invasion and metastasis via the integrin β1/FAK/Akt-MMP9 signaling pathway is shown in Figure 7h.

## DISCUSSION

It has been recently reported that SIPA1 exhibits increased expression in colorectal cancer, melanoma and prostate cancer cells, and indirectly functions to affect tumor cell adhesion and invasion,[16,21,22] but a detailed mechanism of how it regulates breast cancer cell invasion remains unclear. In this study, we showed that SIPA1 was highly expressed in both invasive breast cancer tissues and the highly invasive breast cancer cell MDA-MB-231, but weakly expressed in normal or less aggressive breast cancer tissue and the MCF7 cell line, which has a less aggressive metastatic behavior. In addition, SIPA1 was found to be located in the cell nucleus of MDA-MB-231 and aggressive tumors, as well as in MCF7 cells overexpressing SIPA1. The knockdown of SIPA1 in MDA-MB 231 cell led to a decrease in cell adhesion and invasion potential. These results suggest that SIPA1 may act as a nuclear factor in the promotion of metastatic behavior. We didn't find any typical DNA-binding domain in SIPA1 (Supplementary Figure 2A), suggesting that SIPA1 probably indirectly regulates integrin β1 promoter transcription. Using sequence alignment and the nuclear localization signal sequence predictor NOD,[34] we found no known nuclear localization signal (Supplementary Figure 2B). However, according to the classification tool Euk-mPloc 2.0 (Shanghai, China),[35] SIPA1 is likely to locate to the cell nucleus (Supplementary Figure 2C). Exploration

for additional partners for SIPA1 gave interesting but as of yet indefinite results. We employed an immnoprecipitation assay using an anti-SIPA1 antibody and visualized the baited proteins by SDS-PAGE and silver staining (Supplementary Figure 3A). Mass spectrometry analysis revealed that the most abundant proteins were involved in regulating gene expression, suggesting that SIPA1 likely interact with proteins involved in gene transcription (Supplementary Figure 3B). We found that the majority of these potential interaction partners are typically localized to the cellular nucleus (Supplementary Figure 3C). How SIPA1 protein is directed to the nucleus and regulates gene expression is still under study.

Integrin β1 has been reported to have key roles in promoting cell invasion. The real-time PCR and ChIP analysis reported in this study suggest that SIPA1 may regulate integrin β1 expression through interaction with its promoter. Here, we demonstrated that SIPA1 could interact with the integrin β1 promoter and regulate its expression, as well as affecting downstream FAK/PI3K-MMP9 signaling. A role for FAK and Akt in the regulation of MMP9 in MDA-MB-231 cells has been previously studied,[33] consistent with our results that FAK and Akt were necessary for MMP9 expression (Supplementary Figures 4A and 4B). In addition, we found that a cell invasion assay showed significantly decreased invasion in the presence of a FAK inhibitor compared with a PI3K inhibitor (Supplementary Figure 4C), possibly due to additional effectors downstream of FAK. Rac is an important molecule that regulates cell migration downstream of FAK.[36] Using a GST pull-down assay, we found Rac1-GTP levels in MDA-MB-231 cells to be higher than that in 231/sh-SIPA1 cells (Supplementary Figure 4D).

Rap1 has a critical role in cellular signaling and functioning, likely regulated in part by Rap1GEFs and Rap1GAPs.[37] Rap1GAP was reported to inhibit thyroid carcinoma and melanoma cell invasion in a Rap1 activation-dependent manner.[38–40] In addition, Rap1GAP expression was shown to inhibit tumor growth while also inducing MMP2 and MMP9 mediated cell invasion in squamous cell carcinomas.[41] SIPA1 has been suggested to be a potential Rap1GAP, able to promote Rap1GTP hydrolysis and prostate cancer cell invasion at least partially through the inhibition of Rap1 mediated cell adhesion.[16] We transfected the active form of Rap1V12 into MDA-MB 231 cells and found that active Rap1 could increase phosphorylation of FAK and Akt (Supplementary Figures 5A and 5B), but no obvious differences in MMP9 expression level or invasive ability of the cells were seen (Supplementary Figures 5C and D). This finding is consistent with the results found in endothelial cells,[42] although we can't exclude a role of Rap1 in breast cancer metastasis.

It has been reported that overexpression of SIPA1 in HeLa cells could inhibit cell adhesion.[43] Moreover, SIPA1 has been reported to promote prostate cancer cell invasion at least partially through inhibition of Rap1 activity and cell adhesion.[16] These findings are in contrast to our results, which suggest that breast cancer cell adhesion may be SIPA1 dependent. Two points should be considered. First, subcellular localization of proteins is integral to their function.[44] Overexpression of SIPA1 in the prostate adenocarcinoma LNCaP cell line was reported to result in primarily cytoplasmic localization of SIPA1 and decreased cell adhesion, possibly due to inactivation of the 'cytosolic' Rap signaling pathway, which 'activates' integrin via RapL without affecting the expression level of integrins in most normal cells.[45,46] The subcellular localization of SIPA1 in LNCaP cells is distinct from what we observed in MDA-MB-231 and MCF7 cells (Figures 2c and g), as well as 231/sh-SIPA1 and HEK293 cells (Figures 5f and h). The apparent difference in these results, therefore, may be attributable to the distinct mechanisms of cytosolic vs nuclear SIPA1 on integrin-mediated cell adhesion, inhibition of integrin function and activation of integrin gene expression. Furthermore, we investigated the localization patterns of SIPA1 in different tumor cell types and SIPA1 predominantly localized to the nucleus was uncommon (Data not shown). Second, protein often have distinct role in different types of cells or tissues in part due to diverse protein expression profiles necessary for their unique cellular functions. Indeed, when we overexpressed *SIPA1* in MCF7 cells, we found that it did not affect integrin β1 promoter activity (Data not shown), which should be due to the relatively high estrogen receptor expression levels in MCF7, as it's been reported that estrogen receptor-β could regulate ITGB1 expression in breast cancer cells.[47] In addition, we also assayed the localization of SIPA1 in HeLa cells and found that both cytoplasmic and nuclear SIPA1 increased markedly upon transfection with *SIPA1*, with the level of nuclear SIPA1 being somewhat higher than that of cytoplasmic SIPA1. However, overexpressed SIPA1 did not affect integrin β1 promoter activity in HeLa cells (Data not shown), suggesting that regulation of SIPA1 on integrin β1 promoter is cell-type dependent.

In conclusion, we report that SIPA1 interacts with the integrin β1 promoter and regulates breast cancer cell migration and invasion via the FAK/Akt-MMP9 signaling pathway. These data suggest that SIPA1 has a pivotal role in integrin-mediated signaling and could be critical in integrin-mediated cell invasion.

## MATERIALS AND METHODS

### Antibodies and reagents

Primary antibodies against phospho-Tyr397 FAK, total FAK, phospho-Ser473 Akt, total Akt, PARP, phospho-Tyr416 Src, total Src, phospho-Erk1/2, total Erk1/2, β-actin were purchased from Cell Signaling Technology (Boston, MA, USA). Antibodies against anti-human SIPA1 (Medical & Biological Laboratories, Nagoya, Japan), integrin β1 (Santa Cruz Biotechnology, Dallas, TX, USA), Rap1 (Santa Cruz Biotechnology), F-actin (Abcam, San Francisco, CA, USA), histone H2A and tubulin (Beyotime Institute of Biotechnology, Haimen, China) and MMP9 Elisa kit (Neobioscience, Shenzhen, China) were obtained from their respective companies. An FAK inhibitor PF573228 was purchased from Tocris Bioscience (Bristol, UK). Wortmannin and MMP9 inhibitor I were purchased from Merck4Biosciences (Darmstadt, Germany).

### Cell lines and tumor samples

MDA-MB-231 cell line was obtained from Kyoto University and was maintained in RPMI-1640 medium (Life Technologies, Carlsbad, CA, USA) supplemented with 10% fetal bovine serum (FBS), 50 IU/ml penicillin and 50 μg/ml streptomycin in 5% $CO_2$ at 37 °C. MCF7 cells were purchased from American Type Culture Collection (ATCC, Manassas, VA, USA) and maintained in Dulbecco's modified Eagle medium instead (Life Technologies). Breast cancer tissue samples were collected from the Department of Pathology of the Hubei Cancer Hospital, Wuhan, China. Informed consent on this study was obtained from each subject. The clinical features of the patients were recorded according to the pathological report. Breast cancer specimen collection and use approved by the Clinical Research Ethics Committee of Hubei Cancer Hospital and Tongji Medical College, Huazhong University of Science and Technology.

### Plasmid, transient transfection and generation of cell lines

SIPA1 knockdown was performed by introducing pSINsi-hU6 (Takara Bio, Shiga, Japan) containing *SIPA1*-specific short hairpin RNA into MDA-MB-231 cells as described previously.[16] After screening, the isolated cell clones with high-efficiency *SIPA1* gene knockdown were maintained in the same condition with original MDA-MB-231 cells. Plasmids containing human *SIPA1* gene, Flag-tagged *Rap1V12* were obtained from Professor Nagahiro Minato (Kyoto University, Japan). Transient overexpression of interested genes was conducted using Lipofectamine 2000 (Invitrogen, Shanghai, China) according to the manufacturer's instruction.

### Immunohistochemistry, quantum dot-based immunofluorescence and histologic scoring

Conventional immunohistochemistry and quantum dot-based immunofluorescent staining of SIPA1 were conducted on clinical sections as previously described.[48] All slides were examined with an Olympus BX51 microscope and images were captured using an Olympus DP71 camera (Olympus Optical, Tokyo, Japan). The immunoreactivity of SIPA1 in the

nucleus was ranked into three groups according to the percentage of the positive tumor cells: high (+++, >30%), low and medium (0–30%), and negative (0%). The immunoreactivity for non-nuclear SIPA1 was scored using the immunoreactivity score system established before.[49]

### RT–PCR and real-time PCR

Cells were collected using Trizol (Invitrogen) reagent followed by RNA extraction according to the manufacturer's instruction. Equal amount of RNA was used for the synthesis of first-strand cDNA. one microliter of reverse transcription product was used as template to amplify interested genes with specific primers. The primers used were as follows: SIPA1: 5′-TGCAAGATGGTGGCAGTCCTC-3′ and 5′-CTGCCCGCCTCCGACATGATC-3′; Integrin-β1: 5′-TTTCGATGCCATCATGCAA-3′ and 5′-ACCAGCAGCCGTGTAACATTC-3′; MMP9: 5′-CGCAGACATCGTCATCCAGT-3′ and 5′-GGATTGGCCTTGGAAGATGA-3′; MMP2: 5′-GCGACAAGAAGTATGGCTTC-3′ and 5′-TGCCAAGGTCAATGTCAGGA-3′; β-actin: 5′-CGGAACCGCTCATTGCC-3′ and 5′-ACCCACACTGTGCCCATCTA-3′. The amplification for real-time PCR was conducted by an Applied Biosystems StepOne real-time PCR system, and relative fold changes were determined using the $2^{-\Delta\Delta CT}$ method as described previously,[50] in which the β-actin was used for normalization.

### Nuclear fractionation and western blotting

Cells were lysed in a lysis buffer (100×: 10 mM HEPES, pH 7.9, 50 mM NaCl, 0.1 mM EDTA, 0.5% Triton×100, 1 mM PMSF) on ice for 10 min. After centrifugation at 1000 r.p.m. for 10 min, cytoplasmic/membrane supernatant was collected into a new tube. Pelleted nuclei were washed in buffer W (10 mM HEPES, pH 7.9, 10 mM KCl, 0.1 mM EDTA, 0.1 mM EGTA, 1 mM PMSF, 1% Cocktail). Then the nuclear extract was collected in buffer N (10 mM HEPES, pH 7.9, 500 mM NaCl, 0.1 mM EDTA, 0.1 mM EGTA, 0.1% NP-40, 1 mM PMSF, 1% Cocktail). Western blotting was performed as previously described.[51]

### Immunofluorescence

Immunostaining was done as previously described.[52] In brief, cells were seeded onto cover glasses placed in 24-well plates, and primary antibodies were incubated for overnight at 4 °C followed by staining with TRITC-coupled secondary antibodies (Protein Tech Group, Chicago, IL, USA) for 1 h at room temperature. Cells were visualized by laser scanning microscopy (Olympus IX71) and imaged with the Andor IQ 2 software (www.andor.com).

### Zymography

The activity of secreted MMP9 was analyzed using gelatin zymography assay as described previously.[53] Cells were seeded to 60 mm dishes. Conditioned media from cultured cells were analyzed by 8% SDS-PAGE gel containing 0.1% (w/v) gelatin (Sigma, St Louis, MO, USA) in nonreducing laemmli's sample buffer. The bands were visualized by using the Coomassie blue staining method.

### Chromatin immunoprecipitation

Protein–DNA crosslinking was performed with a formaldehyde treatment (1.42% final concentration). The immunoprecipitation was conducted as described previously,[54] with the exception of the DNA purification process: the complex of protein–DNA beads was washed in elution buffer (100 μl 10% SDS, 100 μl 1 M $NaHCO_3$, 800 μl $H_2O$, total 1 ml) and supernatants were collected. DNA was purified using a DNA recovery kit (Tiangen Biotech, Beijing, China) and analyzed by PCR using the primer for integrin β1 promoter: Forward, 5′-CATCTCGGAAGCCCCCTGAGTC-3′; Reverse, 5′-TCCCCAGTCTCACCACCCTTCGT-3′.

### Luciferase reporter assay

ITGB1 promoter sequence was cloned into a pGL-4 basic luciferase expression vector (Promega, Madison, WI, USA) as described previously.[55] Reporter assays were performed in cells transfected with the indicated promoter constructs and analyzed using Dual-Luciferase Reporter Assay Kit (Promega). The activity of luciferases was measured by GloMax 20/20 Luminometer (Promega). All activity was normalized with respect to cotransfected Renilla plasmid.

### Cell proliferation assay

Cell growth ability *in vitro* was measured as described previously.[56]

### Soft-agar assay

To evaluate the anchorage-independent growth ability, soft-agar assay was employed as used before.[57] In brief, 0.75% agar support of the bottom was prepared in RPMI-1640 containing 10% FBS using a 60-mm dish. $3\times10^4$ Cells were collected, washed and mixed with the top-agarose suspension at a final concentration of 0.35%, which was then layered onto the bottom agar. After incubated at 37 °C for 18 days, the colonies were stained with solution containing 0.04% crystal violet and 2% ethanol, and images were taken. Colonies from three replicate dishes of each sample were counted.

### Scratch assay

Cell scratch assay was conducted following a published protocol.[58]

### Cell adhesion assay

Assessment of cell adhesion to ECM was conducted as described previously.[20] The plates were coated with 5 μg/ml fibronectin (Sigma) or Matrigel (BD Biosciences, San Jose, CA, USA) before seeding the cells. To study cell adhesion to endothelial cells, HUVECs were seeded onto a 24-well plate and allowed to form a fully confluent layer. MDA-MB-231 cells were incubated in RPMI-1640 medium containing 2 μg/ml of the fluorescent dye DiI (Sigma) at 37 °C for 30 min. HUVECs were washed three times before the dye-loaded cells were added and incubated at 37 °C for 30 min. Cell suspensions were withdrawn and fluorescent images were obtained (Leica, Solms, Germany). Fluorescent areas after normalized to each cell morphology area were used for quantification analysis.

### Transwell migration and invasion assay

Cell migration was analyzed *in vitro* using Transwell Permeable Supports (Corning, New York, NY, USA). In brief, cells were seeded into each insert of the 24-well plate and incubated at 37 °C for 24 h. After removal of the cells on the upper side of the membrane with cotton swabs, the cells on the bottom side of the membrane were fixed with methanol for 10 min followed by staining with crystal violet for 5 min. After washing with distilled water, the invaded cells on the membrane were counted in three random fields of view per transwell, and images were captured by a microscope containing a CCD camera (Miotic, Xiamen, China). A similar procedure using the Transwell insert precoated with 80 μg Matrigel was performed to measure the ability of cell invasion.

### Animal care and xenografts

Transgenic Tg (flk1:EGFP) zebrafish (generously given by the Institute of Hydrobiology, Chinese Academy of Sciences, Wuhan, China) were kept at 28 °C in aquaria with 14/10 day/night light cycles. Cells were labeled with DiI as above. A total of 500 cells were injected into the perivitelline space of 48- hour post-fertilization embryos using a microinjector (World Precision Instruments, Sarasota, FL, USA). Embryos were incubated at 28 °C for 3 days and imaged by fluorescent microscope (Olympus).

### Statistical analysis

A two-tailed Student's *t*-test was used when comparing the means of two groups (GraphPad Prism, San Diego, CA, USA). If not otherwise indicated, $^*P<0.05$; $^{**}P<0.01$; $^{***}P<0.001$. The associations between nuclear SIPA1 expression and metastatic lymph node status, and the association of total SIPA1 expression with nuclear-expressed SIPA1 protein in breast cancer tissues were assessed using the Freeman–Halton extension of the Fisher exact probability test (two sided).[59]

## CONFLICT OF INTEREST

The authors declare no conflict of interest.

## ACKNOWLEDGEMENTS

This work was supported partly by grants of National Basic Research Program of China (2011CB910401), NSFC (31271504) and 2009DFA31940 from The Ministry of Science and Technology, China.

## DISCLAIMER

The funders had no role in study design, data collection and analysis, decision to publish or preparation of the manuscript.

## REFERENCES

1 Redig AJ, McAllister SS. Breast cancer as a systemic disease: a view of metastasis. *J Intern Med* 2013; **274**: 113–126.
2 Colzani E, Liljegren A, Johansson AL, Adolfsson J, Hellborg H, Hall PF *et al.* Prognosis of patients with breast cancer: causes of death and effects of time since diagnosis, age, and tumor characteristics. *J Clin Oncol* 2011; **29**: 4014–4021.
3 Valastyan S, Weinberg RA. Tumor metastasis: molecular insights and evolving paradigms. *Cell* 2011; **147**: 275–292.
4 Drukker CA, Bueno-de-Mesquita JM, Retel VP, van Harten WH, van Tinteren H, Wesseling J *et al.* A prospective evaluation of a breast cancer prognosis signature in the observational RASTER study. *Int J Cancer* 2013; **133**: 929–936.
5 Kurachi H, Wada Y, Tsukamoto N, Maeda M, Kubota H, Hattori M *et al.* Human SPA-1 gene product selectively expressed in lymphoid tissues is a specific GTPase-activating protein for Rap1 and Rap2. Segregate expression profiles from a rap1GAP gene product. *J Biol Chem* 1997; **272**: 28081–28088.
6 Valles AM, Beuvin M, Boyer B. Activation of Rac1 by paxillin-Crk-DOCK180 signaling complex is antagonized by Rap1 in migrating NBT-II cells. *J Biol Chem* 2004; **279**: 44490–44496.
7 Gao L. Ras-Associated protein-1 regulates extracellular signal-regulated kinase activation and migration in melanoma cells: two processes important to melanoma tumorigenesis and metastasis. *Cancer Res* 2006; **66**: 7880–7888.
8 Lyle KS, Raaijmakers JH, Bruinsma W, Bos JL, de Rooij J. cAMP-induced Epac-Rap activation inhibits epithelial cell migration by modulating focal adhesion and leading edge dynamics. *Cell signalling* 2008; **20**: 1104–1116.
9 Bailey CL, Kelly P, Casey PJ. Activation of Rap1 promotes prostate cancer metastasis. *Cancer Res* 2009; **69**: 4962–4968.
10 Malchinkhuu E, Sato K, Maehama T, Ishiuchi S, Yoshimoto Y, Mogi C *et al.* Role of Rap1B and tumor suppressor PTEN in the negative regulation of lysophosphatidic acid-induced migration by isoproterenol in glioma cells. *Mol. Biol Cell* 2009; **20**: 5156–5165.
11 Hernandez-Varas P, Colo GP, Bartolome RA, Paterson A, Medrano-Fernandez I, Arellano-Sanchez N *et al.* Rap1-GTP-interacting adaptor molecule (RIAM) protein controls invasion and growth of melanoma cells. *J Biol Chem* 2011; **286**: 18492–18504.
12 McSherry EA, Brennan K, Hudson L, Hill AD, Hopkins AM. Breast cancer cell migration is regulated through junctional adhesion molecule-A-mediated activation of Rap1 GTPase. *Breast Cancer Res* 2011; **13**: R31.
13 Park YG, Zhao X, Lesueur F, Lowy DR, Lancaster M, Pharoah P *et al.* Sipa1 is a candidate for underlying the metastasis efficiency modifier locus Mtes1. *Nature Genet* 2005; **37**: 1055–1062.
14 Crawford NP, Ziogas A, Peel DJ, Hess J, Anton-Culver H, Hunter KW. Germline polymorphisms in SIPA1 are associated with metastasis and other indicators of poor prognosis in breast cancer. *Breast Cancer Res* 2006; **8**: R16.
15 Farina A, Hattori M, Qin J, Nakatani Y, Minato N, Ozato K. Bromodomain protein Brd4 binds to GTPase-activating SPA-1, modulating its activity and subcellular localization. *Mol Cell Biol* 2004; **24**: 9059–9069.
16 Shimizu Y, Hamazaki Y, Hattori M, Doi K, Terada N, Kobayashi T *et al.* SPA-1 controls the invasion and metastasis of human prostate cancer. *Cancer Sci* 2011; **102**: 828–836.
17 Alsarraj J, Faraji F, Geiger TR, Mattaini KR, Williams M, Wu J *et al.* BRD4 short isoform interacts with RRP1B, SIPA1 and components of the LINC complex at the inner face of the nuclear membrane. *PloS One* 2013; **8**: e80746.
18 Crawford NP, Alsarraj J, Lukes L, Walker RC, Officewala JS, Yang HH *et al.* Bromodomain 4 activation predicts breast cancer survival. *Proc Natl Acad Sci USA* 2008; **105**: 6380–6385.
19 Alsarraj J, Walker RC, Webster JD, Geiger TR, Crawford NP, Simpson RM *et al.* Deletion of the proline-rich region of the murine metastasis susceptibility gene Brd4 promotes epithelial-to-mesenchymal transition- and stem cell-like conversion. *Cancer Res* 2011; **71**: 3121–3131.
20 Su L, Hattori M, Moriyama M, Murata N, Harazaki M, Kaibuchi K *et al.* AF-6 controls integrin-mediated cell adhesion by regulating Rap1 activation through the specific recruitment of Rap1GTP and SPA-1. *J Biol Chem* 2003; **278**: 15232–15238.
21 Ji K, Ye L, Toms AM, Hargest R, Martin TA, Ruge F *et al.* Expression of signal-induced proliferation-associated gene 1 (SIPA1), a RapGTPase-activating protein, is increased in colorectal cancer and has diverse effects on functions of colorectal cancer cells. *Cancer Genomics Proteomics* 2012; **9**: 321–327.
22 Mathieu V, Pirker C, Schmidt WM, Spiegl-Kreinecker S, Lotsch D, Heffeter P *et al.* Aggressiveness of human melanoma xenograft models is promoted by aneuploidy-driven gene expression deregulation. *Oncotarget* 2012; **3**: 399–413.
23 Marques IJ, Weiss FU, Vlecken DH, Nitsche C, Bakkers J, Lagendijk AK *et al.* Metastatic behaviour of primary human tumours in a zebrafish xenotransplantation model. *BMC cancer* 2009; **9**: 128.
24 Guo W, Giancotti FG. Integrin signalling during tumour progression. *Nature reviews Molecular cell biology* 2004; **5**: 816–826.
25 Sahai E. Mechanisms of cancer cell invasion. *Curr Opin Genet Dev* 2005; **15**: 87–96.
26 Cavallaro U, Christofori G. Cell adhesion and signalling by cadherins and Ig-CAMs in cancer. *Nat Rev Cancer* 2004; **4**: 118–132.
27 Ruoslahti E. Fibronectin and its integrin receptors in cancer. *Adv Cancer Res* 1999; **76**: 1–20.
28 Hood JD, Cheresh DA. Role of integrins in cell invasion and migration. *Nat Rev Cancer* 2002; **2**: 91–100.
29 Mitra SK, Schlaepfer DD. Integrin-regulated FAK-Src signaling in normal and cancer cells. *Curr Opin Cell Biol* 2006; **18**: 516–523.
30 Mitra SK, Hanson DA, Schlaepfer DD. Focal adhesion kinase: in command and control of cell motility. *Nat Rev Mol Cell Biol* 2005; **6**: 56–68.
31 Maity G, Fahreen S, Banerji A, Roy Choudhury P, Sen T, Dutta A *et al.* Fibronectin-integrin mediated signaling in human cervical cancer cells (SiHa). *Mol Cell Biochem* 2010; **336**: 65–74.
32 Sen T, Dutta A, Maity G, Chatterjee A. Fibronectin induces matrix metalloproteinase-9 (MMP-9) in human laryngeal carcinoma cells by involving multiple signaling pathways. *Biochimie* 2010; **92**: 1422–1434.
33 Maity G, Choudhury PR, Sen T, Ganguly KK, Sil H, Chatterjee A. Culture of human breast cancer cell line (MDA-MB-231) on fibronectin-coated surface induces pro-matrix metalloproteinase-9 expression and activity. *Tumour Biol* 2011; **32**: 129–138.
34 Scott MS, Troshin PV, Barton GJ. NoD: a Nucleolar localization sequence detector for eukaryotic and viral proteins. *BMC Bioinformatics* 2011; **12**: 317.
35 Chou KC, Shen HB. A new method for predicting the subcellular localization of eukaryotic proteins with both single and multiple sites: Euk-mPLoc 2.0. *PloS One* 2010; **5**: e9931.
36 Carragher NO, Frame MC. Focal adhesion and actin dynamics: a place where kinases and proteases meet to promote invasion. *Trends Cell Biol* 2004; **14**: 241–249.
37 Bos JL, Rehmann H, Wittinghofer A. GEFs and GAPs: critical elements in the control of small G proteins. *Cell* 2007; **129**: 865–877.
38 Tsygankova OM, Prendergast GV, Puttaswamy K, Wang Y, Feldman MD, Wang H *et al.* Downregulation of Rap1GAP contributes to Ras transformation. *Mol Cell Biol* 2007; **27**: 6647–6658.
39 Zuo H, Gandhi M, Edreira MM, Hochbaum D, Nimgaonkar VL, Zhang P *et al.* Downregulation of Rap1GAP through epigenetic silencing and loss of heterozygosity promotes invasion and progression of thyroid tumors. *Cancer Res* 2010; **70**: 1389–1397.
40 Zheng H, Gao L, Feng Y, Yuan L, Zhao H, Cornelius LA. Down-regulation of Rap1GAP via promoter hypermethylation promotes melanoma cell proliferation, survival, and migration. *Cancer Res* 2009; **69**: 449–457.
41 Mitra RS, Goto M, Lee JS, Maldonado D, Taylor JM, Pan Q *et al.* Rap1GAP promotes invasion via induction of matrix metalloproteinase 9 secretion, which is associated with poor survival in low N-stage squamous cell carcinoma. *Cancer Res* 2008; **68**: 3959–3969.
42 Carmona G, Gottig S, Orlandi A, Scheele J, Bauerle T, Jugold M *et al.* Role of the small GTPase Rap1 for integrin activity regulation in endothelial cells and angiogenesis. *Blood* 2009; **113**: 488–497.
43 Tsukamoto N, Hattori M, Yang H, Bos JL, Minato N. Rap1 GTPase-activating protein SPA-1 negatively regulates cell adhesion. *J Biol Chem* 1999; **274**: 18463–18469.
44 Hung MC, Link W. Protein localization in disease and therapy. *J Cell Sci* 2011; **124**: 3381–3392.
45 Katagiri K, Maeda A, Shimonaka M, Kinashi T. RAPL, a Rap1-binding molecule that mediates Rap1-induced adhesion through spatial regulation of LFA-1. *Nat Immunol* 2003; **4**: 741–748.
46 Bivona TG, Wiener HH, Ahearn IM, Silletti J, Chiu VK, Philips MR. Rap1 up-regulation and activation on plasma membrane regulates T cell adhesion. *J Cell Biol* 2004; **164**: 461–470.
47 Lindberg K, Strom A, Lock JG, Gustafsson JA, Haldosen LA, Helguero LA. Expression of estrogen receptor beta increases integrin alpha1 and integrin beta1 levels and enhances adhesion of breast cancer cells. *J Cell Physiol* 2010; **222**: 156–167.
48 Chen C, Peng J, Xia HS, Yang GF, Wu QS, Chen LD *et al.* Quantum dots-based immunofluorescence technology for the quantitative determination of HER2 expression in breast cancer. *Biomaterials* 2009; **30**: 2912–2918.
49 Camp RL, Rimm EB, Rimm DL. Met expression is associated with poor outcome in patients with axillary lymph node negative breast carcinoma. *Cancer* 1999; **86**: 2259–2265.

50 Cayrol C, Clerc P, Bertrand C, Gigoux V, Portolan G, Fourmy D *et al.* Cholecystokinin-2 receptor modulates cell adhesion through beta 1-integrin in human pancreatic cancer cells. *Oncogene* 2006; **25**: 4421–4428.
51 Tu H, Xu C, Zhang W, Liu Q, Rondard P, Pin JP *et al.* GABAB receptor activation protects neurons from apoptosis via IGF-1 receptor transactivation. *J Neurosci* 2010; **30**: 749–759.
52 Hsu TI, Wang MC, Chen SY, Yeh YM, Su WC, Chang WC *et al.* Sp1 expression regulates lung tumor progression. *Oncogene* 2012; **31**: 3973–3988.
53 Liu JF, Crepin M, Liu JM, Barritault D, Ledoux D. FGF-2 and TPA induce matrix metalloproteinase-9 secretion in MCF-7 cells through PKC activation of the Ras/ERK pathway. *Biochem Biophys Res Commun* 2002; **293**: 1174–1182.
54 Nelson JD, Denisenko O, Bomsztyk K. Protocol for the fast chromatin immunoprecipitation (ChIP) method. *Nat Protocol* 2006; **1**: 179–185.
55 Keely S, Glover LE, MacManus CF, Campbell EL, Scully MM, Furuta GT *et al.* Selective induction of integrin beta1 by hypoxia-inducible factor: implications for wound healing. *FASEB J* 2009; **23**: 1338–1346.
56 Mizugaki H, Sakakibara-Konishi J, Ikezawa Y, Kikuchi J, Kikuchi E, Oizumi S *et al.* gamma-Secretase inhibitor enhances antitumour effect of radiation in Notch-expressing lung cancer. *Br J Cancer* 2012; **106**: 1953–1959.
57 Kunapuli P, Chitta KS, Cowell JK. Suppression of the cell proliferation and invasion phenotypes in glioma cells by the LGI1 gene. *Oncogene* 2003; **22**: 3985–3991.
58 Liang CC, Park AY, Guan JL. *In vitro* scratch assay: a convenient and inexpensive method for analysis of cell migration *in vitro*. *Nat Protocols* 2007; **2**: 329–333.
59 Freeman GH, Halton JH. Note on an exact treatment of contingency, goodness of fit and other problems of significance. *Biometrika* 1951; **38**: 141–149.

Supplementary Information accompanies this paper on the Oncogene website (http://www.nature.com/onc)

SCIENTIFIC REPORTS

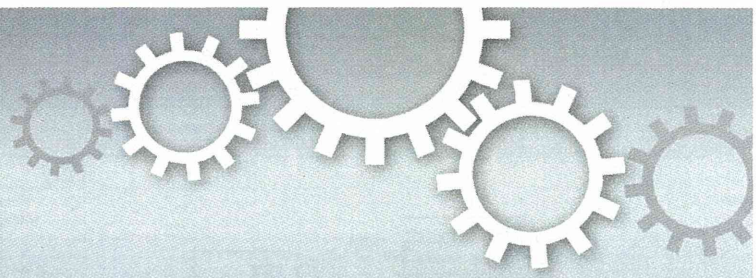

OPEN

SUBJECT AREAS:
ACUTE LYMPHOCYTIC LEUKAEMIA
LEUKAEMIA

Received
23 July 2014

Accepted
23 December 2014

Published
23 January 2015

Correspondence and requests for materials should be addressed to N.M. (minato@imm.med.kyoto-u.ac.jp)

# Crucial role of the Rap G protein signal in Notch activation and leukemogenicity of T-cell acute lymphoblastic leukemia

Keiko Doi[1], Takahiko Imai[1], Christopher Kressler[1], Hideo Yagita[2], Yasutoshi Agata[1], Marc Vooijs[3], Yoko Hamazaki[1], Joe Inoue[1] & Nagahiro Minato[1]

[1]Department of Immunology and Cell Biology, Graduate School of Medicine, Kyoto University, Sakyo-ku, Kyoto, Japan, [2]Department of Immunology, Juntendo University School of Medicine, Bunkyo-ku, Tokyo, Japan, [3]Maastricht Radiation Oncology and School for Oncology and Developmental Biology, University of Maastricht, Maastricht, The Netherlands.

**The Rap G protein signal regulates Notch activation in early thymic progenitor cells, and deregulated Rap activation ($Rap^{high}$) results in the development of Notch-dependent T-cell acute lymphoblastic leukemia (T-ALL). We demonstrate that the Rap signal is required for the proliferation and leukemogenesis of established Notch-dependent T-ALL cell lines. Attenuation of the Rap signal by the expression of a dominant-negative Rap1A17 or Rap1GAP, Sipa1, in a T-ALL cell line resulted in the reduced Notch processing at site 2 due to impaired maturation of Adam10. Inhibition of the Rap1 prenylation with a geranylgeranyl transferase inhibitor abrogated its membrane-anchoring to Golgi-network and caused reduced proprotein convertase activity required for Adam10 maturation. Exogenous expression of a mature form of Adam10 overcame the Sipa1-induced inhibition of T-ALL cell proliferation. T-ALL cell lines expressed Notch ligands in a Notch-signal dependent manner, which contributed to the cell-autonomous Notch activation. Although the initial thymic blast cells barely expressed Notch ligands during the T-ALL development from $Rap^{high}$ hematopoietic progenitors in vivo, the ligands were clearly expressed in the T-ALL cells invading extrathymic vital organs. These results reveal a crucial role of the Rap signal in the Notch-dependent T-ALL development and the progression.**

The Notch signal is essential for thymic T-cell development[1,2]. Notch protein is synthesized as a large single peptide, which is later cleaved intracellularly at a heterodimerization (HD) domain (S1 cleavage) to generate the heterodimeric Notch receptor[3]. Upon engagement with specific ligands, the Notch receptor is activated through successive proteolytic cleavages at a juxtamembrane site (S2) followed by an intramembranous site (S3) mediated by Adam10 and γ-secretase complex, respectively, resulting in the release and nuclear translocation of Notch intracellular domain (NICD)[4]. In early T-cell progenitors (ETPs), Notch receptor is activated via Delta-like 4 (Dll4), which is expressed on thymic epithelial cells[5]. The Notch signal also plays a key role in the development of T-cell acute lymphoblastic leukemia (T-ALL)[6]. More than 50% of human T-ALL cell lines show "activating" *Notch1* mutations[7], although more recent studies suggest that these mutations may not alone suffice for T-ALL development[8–10].

We have reported that the Rap G protein signal also plays an important part in thymic T-cell development as well as T-ALL genesis[11–13]. The signal switch function of Rap is regulated positively by specific guanine nucleotide exchange factors such as C3G and negatively by GTPase-activating proteins represented by Sipa1[12]. Impaired Rap activation in ETPs results in arrested thymic T-cell development, whereas deregulated Rap activation ($Rap^{high}$) remarkably enhances the Notch-dependent proliferation of ETPs[11]. Moreover, bone marrow transplantation (BMT) of $Rap^{high}$ hematopoietic progenitor cells (HPCs) results in the development of T-ALL[13]. Intriguingly, such T-ALL cells were dependent on the Notch signal and often showed characteristic *Notch1* mutations similar to human T-ALL[13], suggesting a functional crosstalk between the Rap and Notch signals.

In current study, we demonstrate that the Rap signal controls Notch activation in T-ALL cells by regulating proprotein convertase activity required for the maturation of Adam10 mediating the Notch processing. We further indicate that the sustained Notch activation in thymic $Rap^{high}$ blast cells eventually results in the expression of Notch ligands, leading to the cell-autonomous Notch activation and systemic T-ALL progression.